

Experimental Investigation of Aerodynamics of a Car Model

A. B. Khoshnevis*

Department of Mechanical Engineering,
Hakim Sabzevari University
E-mail: Khosh1966@yahoo.com

V. Barzanooni

Department of Mechanical Engineering,
Hakim Sabzevari University
E-mail: Mrvahid4154@yahoo.com

F. Foroozesh

Department of Mechanical Engineering,
Hakim Sabzevari University
Email: foroozesh_fa@yahoo.com

Received: 27 November 2011, Revised: 19 July 2011, Accepted: 6 May 2012

Abstract: In this study, the time-average velocity in the near wake of a two-dimensional Notch-Back car model located in the wake of a trailer has been investigated. Experiments were carried out in an open circuit low-speed wind tunnel made by FaraSanjeshSaba Ltd, in Iran. Results show that at close spacing, time-average velocity profile behind the car has a maximum peak due to the interaction of the jet fluid with the wake of the car, such that with increased vehicle spacing, the jet fluid effect creating the maximum velocity peak gradually fades. In addition, along with increasing vehicle spacing, the velocity in the wake of the car starts to grow quickly. To measure the drag coefficient it was preferred to use the wake-survey method combined with the equation recently derived by Van Dam. The dimensionless distance between vehicles derived is based on the length of the front vehicle ranging from 0.1 to 3. It was observed that the car drag coefficient experiences a rising trend at the beginning and then descending along dimensionless distance of 0.1 to 1.3, compared to the individual case. In farther distances it will be less pronounced than the individual case.

Keywords: Experiment, Turbulence, Vehicles, Wake, Wind Tunnel

Reference: Khoshnevis, A. B., Barzanooni, V., Foroozesh, F., "Experimental Investigation of the Aerodynamic of a Car Model", Int J of Advanced Design and Manufacturing Technology, Vol. 6/No. 1, 2013, pp. 41-48.

Biographical notes: **A. B. Khoshnevis** is an associate professor of Mechanical Engineering at Hakim Sabzevari University, Sabzevar, Iran. He received his PhD from Indian Institute of Technology of Madras Chennai (2000), India, MSc from Indian Institute of Technology of Madras Chennai (1995), and BSc from Ferdowsi University of Mashad Iran (1990), all in mechanical engineering. His scientific interest includes experimental aerodynamic. **V. Barzanooni** is MSc student at Faculty of Engineering of Hakim Sabzevari University. **F. Foroozesh** has been MSc student at the Faculty of Engineering of Hakim Sabzevari University from 2008-2011.

2 EXPERIMENTAL SET UP AND MEASUREMENT TECHNIQUE

Present experiments were carried out in an open circuit low-speed wind tunnel to simulate uniform air flow. This wind tunnel has a settling chamber with 4 series of mesh screen (1mm^2) and one honey comb by which to make the airflow uniform. The maximum wind tunnel speed is approximately 30 m/s, with 1800 mm length and $0.4 \times 0.4\text{m}^2$ test area cross-section. The free fluid turbulence intensity is less than 0.1 %. The hotwire used in this study was CTA type, which was manufactured by FaraSanjeshSaba Ltd. Schematic view of the wind tunnel is presented in Figure 1.

Some researchers like Gilli and Chometon [3] or Hanaoka and Kiyohira [4] simulated the above mentioned model numerically. Since the results published by Ahmed are limited, comparable criterion for numerical results were limited to drag coefficient. Gillieron and Spohn [5], and Lienhart and Stooks [6] simulated these models in detail and obtained experimental results including velocity vectors and Reynolds numbers by means of LDA (Laser Doppler Anemometer). Khalighi et al. [7] obtained velocity profiles and turbulent intensity profiles for a car model experimentally.

Javareshkian et al. [8] studied the influence of some parameters on the drag coefficient. Shayesteh [9] tried to study a car model numerically, where Javareshkian et al. [10] studied the same car model experimentally and numerically. Likewise Watkins and Vino [11] studied variation of drag and lift coefficients for Ahmed's models in tandem arrangement. But nowadays, since the common car types are often Notch-Back, hence it is preferred to study such car type in the present research. The wind tunnel implemented is manufactured by FaraSanjeshSabaCompany, which measures fluctuations up to 30 KHz and the accuracy of probe traverse is about 0.1mm.

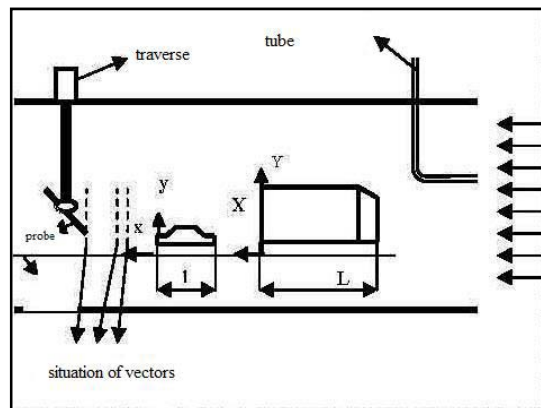


Fig. 2 Schematic view of the experimental apparatus

With respect to the present experimental conditions, a ratio of 0.09 is chosen in this research, where the scale factor of the model decided to be 1-75. Initially, the car model was subjected to air flow independently, and then the test was repeated for the car model at 0.3, 0.4, 0.6, 0.8, 1, 1.3, 2.3, and 3.3 times the length of trailer behind it. Subsequently the data acquisition took place at distances of 0.01, 0.25, 0.5, 0.75, 1, 1.25, and 1.5 times the car length behind the car model (Fig. 2).

3 VALIDATION

In order to ensure the correct operation of the wind tunnel, the validation test was performed. For this purpose, the free stream flow was measured and the velocity profile was observed to be uniform as shown in Fig. 3.

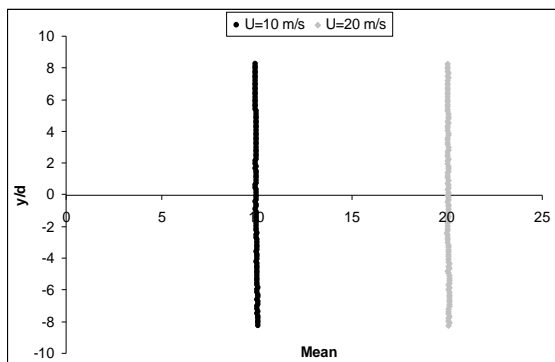


Fig. 3 Average speed fluctuation in the wind tunnel for speeds of 10 and 20 m/s

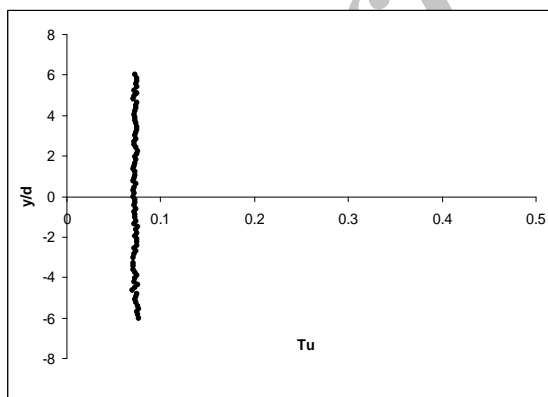


Fig. 4 Turbulence intensity variation in the wind tunnel at a speed of 10 m/s

Another experiment was conducted to measure the free stream turbulence intensity at different wind tunnel speeds (Fig.4). According to the disturbance graphs of the wind tunnel test section; the intensity of turbulence was investigated to be 0.08 %.

Moreover, to survey the accuracy and performance of the wind tunnel and hot-wire anemometer, sample data was obtained and compared with the results claimed by other researchers. However, due to the fact that there was no similar investigation in the literature on the chosen model, therefore a cubic cylinder model was used instead.

Profile of the mean time of the longitudinal velocity component along the main stream (\bar{U}) for a sample cubic cylinder with aspect ratio of $b/h=1$ and Reynolds number of 8600, in two different sections is presented in Fig. 5.

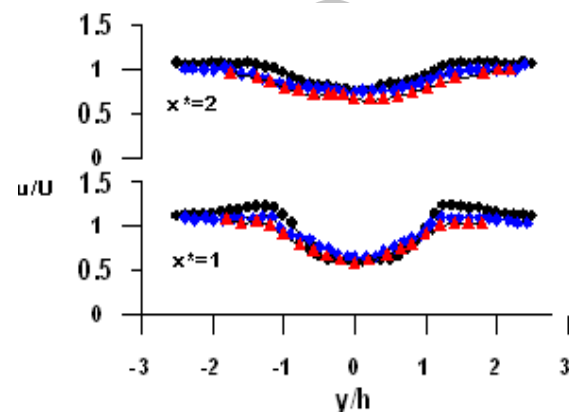


Fig. 5 Profile of mean velocity for a square cylinder in two different sections

As it is observed in Fig. 5, a relatively good conformity exists between the present results and the results claimed by Saha et al. [12] and also by Shadaram et al. [13]; where both have achieved the same Reynolds number.

4 WAKE-SURVEY EQUATIONS

The equations used to measure the drag force, can be simply derived from momentum and continuity equations. Chao [14], Antonia [15] and Van Dam [16] have conducted vast researches on the effect of turbulence intensity on drag coefficient measurement. Van Dam [16] obtained an equation to measure drag coefficient in which Reynolds tensions terms and flow intensity existed, but changes of flow density and viscous term ($\mu \frac{\partial u}{\partial x}$) were ignored. The equation is:

$$C_d = \int \left(\frac{P_{s,a} - P_{s,w}}{q_\infty} \right) d\left(\frac{y}{l}\right) + 2 \int \frac{\bar{u}}{u_\infty} \left(1 - \frac{\bar{u}}{u_\infty} \right) d\left(\frac{y}{l}\right) - 2 \int \frac{\bar{u}^2}{U^2} d\left(\frac{y}{l}\right) \quad (1)$$

Including:

Pressure term: $\int \left(\frac{P_{s,a} - P_{s,w}}{q_w} \right) d\left(\frac{y}{l}\right)$

Momentum term: $2 \int \frac{\bar{u}}{U_\infty} \left(1 - \frac{\bar{u}}{U_\infty} \right) d\left(\frac{y}{l}\right)$

Reynolds tension: $2 \int \frac{\bar{u}'^2}{U_\infty^2} d\left(\frac{y}{l}\right)$

However, based on the analysis of Goldstein [17]:

$$P_{s,a} = P_{s,w} + \bar{q} \quad (2)$$

$$\bar{q} = \frac{1}{2} \rho (\bar{u}'^2 + \bar{v}'^2 + \bar{w}'^2) \quad (3)$$

Substituting equation (3) into equation (1):

$$C_d = 2 \int \sqrt{\frac{\bar{q}}{q_\infty}} \left(1 - \sqrt{\frac{\bar{q}}{q_\infty}} \right) d\left(\frac{y}{l}\right) + \frac{1}{3} \int \frac{(\bar{u}'^2 + \bar{v}'^2 + \bar{w}'^2)}{U_\infty^2} d\left(\frac{y}{l}\right) \quad (4)$$

If $u' = v' = w'$, then

$$C_d = 2 \int \sqrt{\frac{\bar{q}}{q_\infty}} \left(1 - \sqrt{\frac{\bar{q}}{q_\infty}} \right) d\left(\frac{y}{l}\right) + \frac{1}{3} \int \frac{\bar{q}}{q_\infty} d\left(\frac{y}{l}\right) \quad (5)$$

In which:

$$\bar{q} = \frac{1}{2} \rho (\bar{u}'^2 + \bar{v}'^2 + \bar{w}'^2) \quad (6)$$

These equations may be used to determine drag coefficient in wind tunnel via Wake-Survey approach. Hence, Eq. (5) was used to measure drag coefficient in the present work.

5 RESULTS AND DISCUSSION

As shown in Fig. 6, with increment of distance behind the car model, velocity defect is decreased and less fluctuation appears on the velocity profiles. It is observed that, at higher velocities this process is more severe such that at a velocity of 25 m/s, car wake vanishes at 6th station while at other velocities the effect of car wake still remains. On the other hand, at the first station ($x^*=0.01$) exactly behind the model, changes in entering velocity does not have any noticeable effect on the wake mean velocity.

However, with increment of distance, and increment of entrance velocity leads to increase in the amount of mean velocity at the wake: as mentioned earlier with increasing velocity, effects wake vanishes quicker. Another point is the existence of maximum velocity

peak at surfaces beneath and near the model. This phenomenon is due to the existence of fluid jet and boundary layer momentum on the surfaces beneath the model.

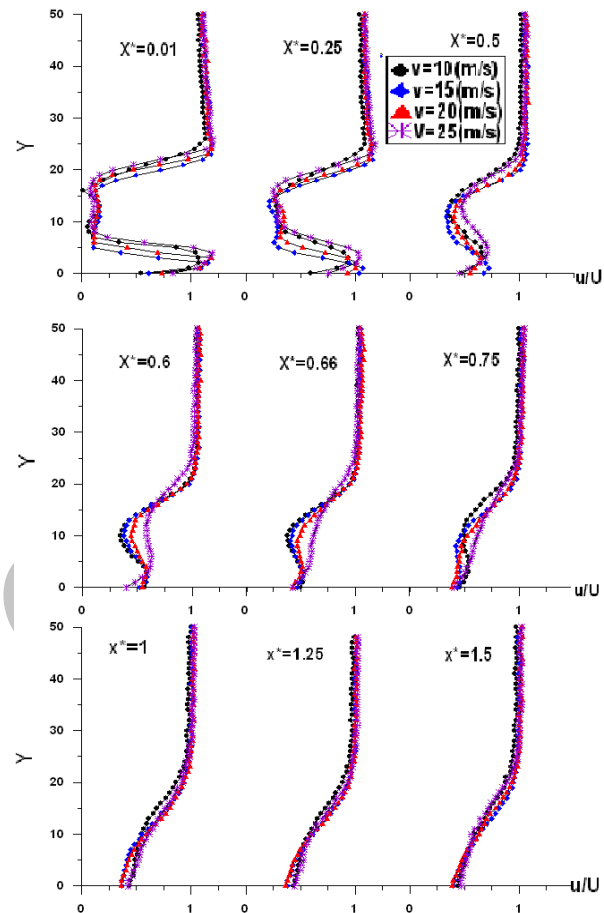


Fig. 6 Mean velocity profiles with respect to the height in different velocities and positions behind the single car.

This may also be explained by the fact that the fluid jet at sections near the model has larger momentum; however by moving away from the model these effects are weakened. Moreover, at sections near the model where the momentum is created at the boundary layer on surface beneath the trailer model, after the boundary layer being vanished, this leads to releasing energy at adjacent regions and eventually growth in flow velocity.

However since this phenomenon happens at a far distances from the model it is not considerable, and it cannot change the particles fluid velocity significantly. In Figures 7 to 13 the mean velocity profiles measured at the wake behind the car model subjected to the wake of the trailer located at several distances is presented and hence compared with a single model.

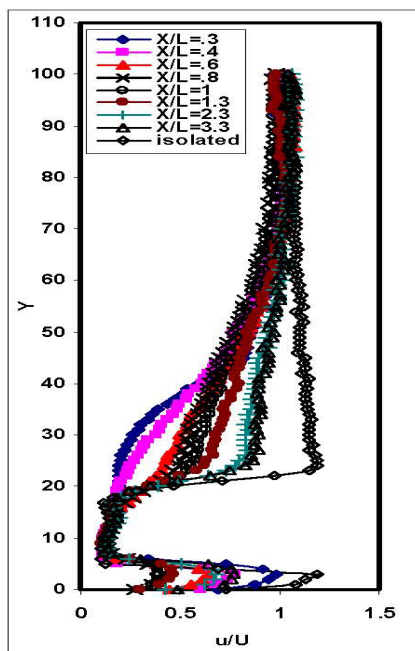


Fig. 7 Mean velocity profiles in the wake of the car subjected to the wake of the trailer($x/l=0.01$)

As shown in Fig. 7 for the first two stations ($x/l=0.3, 0.4$) the car is completely situated in the wake of the trailer and shear layers separated from trailer's roof fall in larger distances behind the car. It is seen that wake velocity increases behind the car, which is predominant with increasing distance between car and trailer. At the last stations the velocity profile almost superposes with the velocity profile of the single car model. In other words, as the effect of trailer wake is being reduced on the car wake, the car gradually departs from the trailer wake.

It is observed that mean velocity behind the car($x/l=0.01$) is almost independent of the car's location and the velocity stays the same. This is in such a way that the fluid jet at sections near the model has larger momentum; however by moving away from the model these effects are weakened. Moreover, at sections near the model where the momentum is created at the boundary layer on surface beneath the trailer model, after the boundary layer being vanished, this leads to releasing energy at adjacent regions and eventually ascent in flow velocity.

The observed peak has an initial decrease due to the increased distance between the car and the trailer but afterwards it increases again. Because of the boundary layer effect on surface beneath the trailer model, maximum velocity peak is less than that of a single car subjected to flow. Increment in distance behind the car model, reduces the influence of the fluid jet and the maximum velocity peak gradually vanishes.

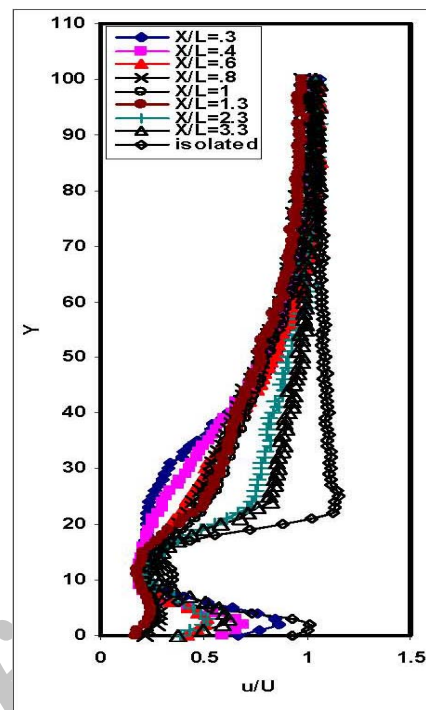


Fig. 8 Mean velocity profiles in the wake of the car subjected to the wake of the trailer($x/l=0.25$)

At the last stations in Figures 12 and 13, maximum velocity peaks are vanished and profiles become more uniform. By locating the car model at the trailer wake, the drag coefficient calculated. Initially, the trailer model was positioned at the test section and by selecting an appropriate control volume, the velocity profile at outlet section was measured. An important point in choosing control volume was to make sure that the inlet and outlet boundaries are far enough so that the pressure at control volume boundaries is the same as ambient pressure.

After the velocity profiles and turbulence intensity were obtained for the outlet section, the drag coefficient of the trailer (which signifies momentum decrement in the control volume) was calculated by Eq. (7). The obtained drag coefficient was 0.477. Next, the car model was positioned at different distances behind the trailer (Fig. 14). For each situation the velocity profiles and turbulence intensities of the outlet section were measured and a unique drag coefficient was obtained for the whole control volume. This coefficient represents the decrement of the control volume momentum caused by compressive and frictional effects of the models. Actually the effects of two models in reducing control volume momentum were obtained. So these effects must be considered. Hence, the trailer drag coefficient calculated before, was subtracted from the total drag coefficient.

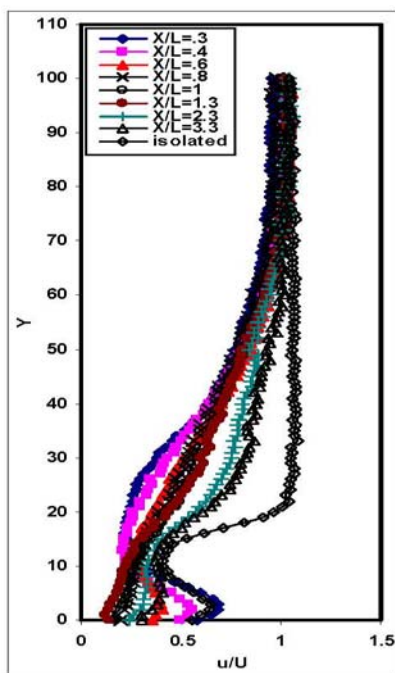


Fig. 9 Mean velocity profiles in the wake of the car subjected to the wake of the trailer($x/l=0.5$)

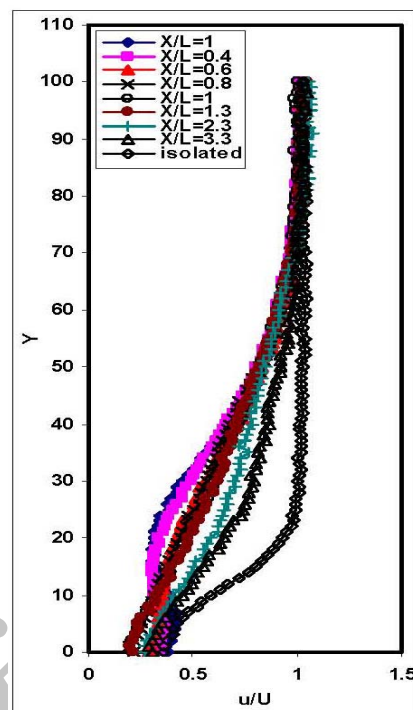


Fig. 11 Mean velocity profiles in the wake of the car subjected to the wake of the trailer($x/l=1$)

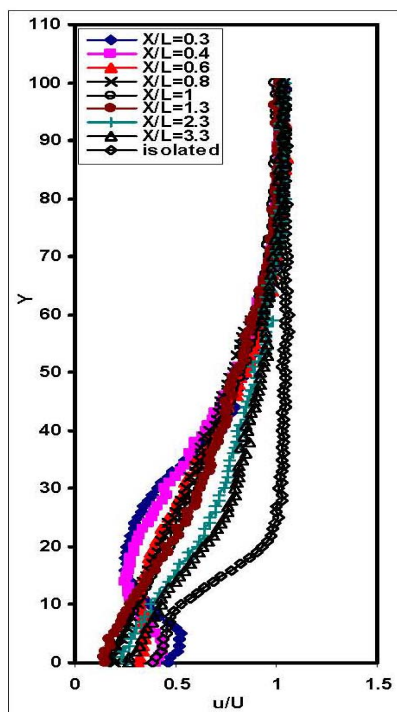


Fig. 10 Mean velocity profiles in the wake of the car subjected to the wake of the trailer($x/l=0.75$)

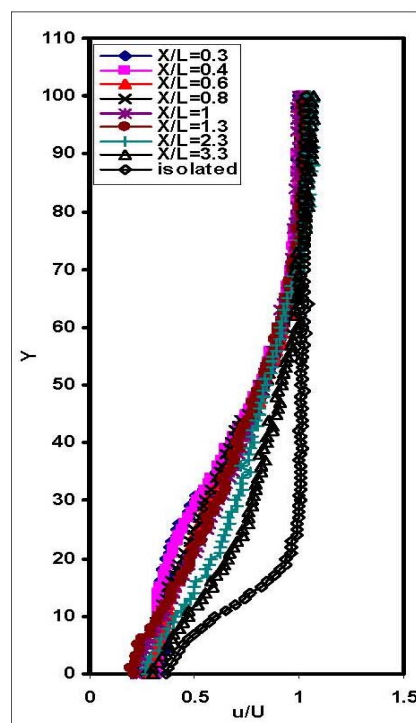


Fig. 12 Mean velocity profiles in the wake of the car subjected to the wake of the trailer($x/l=1.25$)

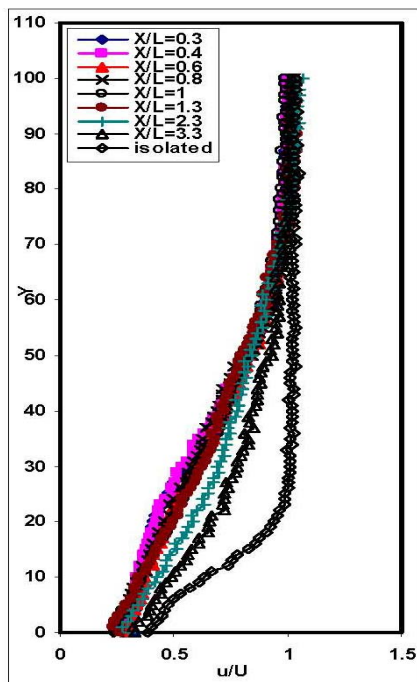


Fig. 13 Mean velocity profiles in wake of car subjected to wake of trailer ($x/l=1.5$)

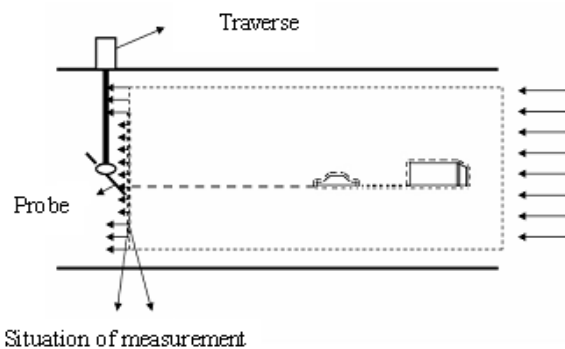


Fig. 14 Schematic view of the vehicle model position following trailer and control volume

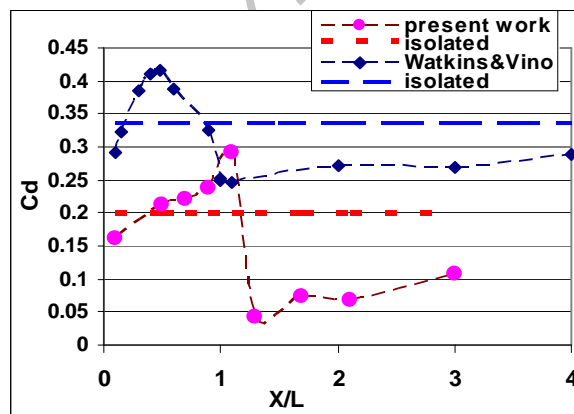


Fig. 15 Variation of vehicle drag coefficients trend compared to previous studies

Fig. 15 shows the drag coefficient values in different positions behind the trailer. It is observed that drag coefficient increases as soon as the distance to the trailer increases. It reaches to a maximum and after a severe drop, reaches to a minimum. Then, as the distance increases more, this value increases gradually, hence diminishing the trailer wake. It is concluded that the main variation of drag coefficient occurs in the range $X/L=1.3$ to 1.1 . The general trend of results is in good agreement to Watkins and Vino [11].

Nevertheless the differences in maximum and minimum ranges of drag coefficient can originate from the difference in the dimensions of the two models undergoing tests. To realize this fact better, the outlet cross section profiles of the velocity defect are displayed in Fig. 16 in which the velocity primarily rises and after a hard drop rises again. This fact confirms the trend of drag coefficient variation too.

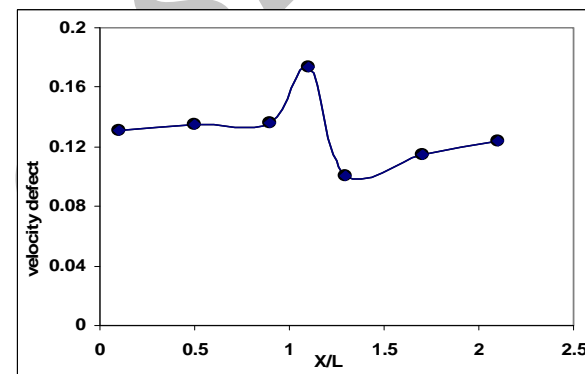


Fig. 16 Velocity defect of outlet section for different positions of the vehicle

6 CONCLUSION

1. When distance between two models is increased, maximum velocity peak gradually decreases due to interaction between the wake and the fluid and vanishes at closer distances to the car model.
2. With increasing vehicle spacing it is observed that the velocity in the wake of the car starts to grow faster.
3. Maximum velocity peak due to the interaction between the wake and the fluid jet exactly behind the car is initially decreased and then afterwards it increases as distance between models is increased.
4. Velocity increment causes an increase in the amount of wake velocity and this increment exceeds as the distance behind car increases.
5. In the dimensionless distance of 0.9 to 1.7, the drag coefficient experiences vast fluctuations.
6. As the distance from the trailer increases, the value of the drag coefficient rises to a maximum peak and then drops severely to a minimum and then rises again.

8 NOMENCLATURE

b:	Width of model
C_d :	Drag coefficient
h:	Model height
L:	Trailer length
l:	Car length
P_t :	Total pressure
P_s :	Static pressure
q:	Dynamic pressure
\bar{q} :	Mean dynamic pressure
Re:	Reynolds number
Tu:	Turbulent intensity level
U:	Free stream velocity
u,v,w:	Velocity component
u', v', w' :	Turbulent velocity component
x:	Distance from car model
X:	Distance from trailer model
ρ :	Density
x^* :	Non-dimensional parameter

REFERENCES

- [1] Hucho, W. H., "Aerodynamics of Road Vehicles, 4th ed.", SAE International, 1998.
- [2] Ahmed, S. R., Ramm, R., and Faltin, G., "Some salient features of The Time-Averaged Ground Vehicle Wake", SAE Technical Paper 840300, 1984, doi:10.4271/840300.
- [3] Gilliéron, P., And Chometon, F., "Modelling of Stationary Three-Dimensional Separated Air Flows around an Ahmed Reference Model", Third International Workshop on Vortex, ESAIM Proceedings, 1999, pp. 92-99.
- [4] Hanaoka, Y., And Kiyohira, A., "Vehicle Aerodynamic Development using PAMFLOW", 1995, pp. 234.
- [5] Gillieron, P., and Spohn, A., "Flow Separations Generated by a Simplified Geometry of an Automotive Vehicle", Journal of wind engineering and industrial aerodynamics, 2002, pp. 724.
- [6] Lienhart, H., and Stoochs, C., "Flow and Turbulence Structures in the Wake of a Simplified Car Model", DGLR FachSymp. Der AG STAB, Stuttgart University, 15-17 Nov., 2000.
- [7] Khalighi, B., Zang, S., Koromilas, C., Balkanyi, S., Bernal, L.P., Iaccarino, G., and Moin, P., "Experimental and computational study of unsteady wake flow behind a body with a drag reduction device", SAE technical paper, 2001, pp. 1001-1024.
- [8] Javarashkian, M. H., Zehsaz, M., and Azar-Khish, A., "Experimental optimization of aerodynamic forces exerted on a vehicle model", 9th International Fluid Dynamics Conference, Shiraz University, 2004.
- [9] Shayesteh, R. "Numerical investigation of aerodynamic forces exerted to a basic model of car", MSc Dissertation, Engineering Department, Tabrizuniversity Publication, 2006.
- [10] DJavarashkian, M. H., Sadafian, R., and Azar-khish, A., "Numerical and Experimental study of flow around a car model of car", Vol.18, No.1, 2006, pp. 49-64.
- [11] Watkins, S., and Vio, G., "The effect of vehicle spacing on the aerodynamics of representative car shape", Journal of wind engineering and industrial aerodynamics, 2008, pp. 1232-1239.
- [12] Saha, A. K., Muralidhar, K., and Biswas, G., "Experimental study of flow past square cylinder at high reynolds numbers", Experiments in Fluids, 2000, pp. 553-563.
- [13] Shadaram, A., Azimi-Fard, M., and Rostamy, N., "Experimental study of characteristics of the flow in the near wake of a rectangular cylinders", Aerospace Mechanics Journal, Vol. 3, No. 3, 2007, pp.13-23.
- [14] Chao, D., and Van Dam, C.P., "Airfoil drag prediction and decomposition", Journal of Aircraft, Vol. 36, No. 4, 1999, pp. 675.
- [15] Antonia, R. A., and Rajagopalan, S., "Determination of drag of a circular cylinder", AIAA Journal, Vol. 28, No. 10, 1990, pp. 1833.
- [16] Van Dam, C. P., "Recent experience with different methods of drag prediction", Progress in Aerospace Science, 35,1999, pp.751-798.
- [17] Goldstein, S., "A note on the measurement of total head and static pressure on a turbulent stream", Proceedings of the Royal Society of London, Series A, Vol. 155,1936, pp. 570-575.